TECHNICAL UNIVERSITY OF CLUJ-NAPOCA

ACTA TECHNICA NAPOCENSIS

Series: Applied Mathematics, Mechanics, and Engineering
Vol. 67, Issue Special IV, August, 2024

ANALYSIS OF THE INFLUENCE OF RINGS MATERIALS AND WORKING CONDITIONS ON THE CONTACT PRESSURE TO A DOUBLE CARTRIDGE MECHANICAL SEAL

Andrei STANCIU, Razvan George RIPEANU

Abstract: *Mechanical seals consists of two rings, one being static and the other one dynamic, which are actioned by one or two fluid pressures, and an elastic force (or magnetic) which keeps the two faces of the rings in permanent contact. The paper is showing how the pressure on contact surface is changing, based on different rings materials, as impregnated graphite with resins, silicon carbide or tungsten carbide, for a double cartridge mechanical seal, using the FEA model of calculation. Based on the type of material pair that is getting in contact, the behavior of the seal face pressure is changing, due to material ability to deform, absorb stress or due to friction coefficient. The parameters of materials were considered alongside both internal and external pressure, pump shaft speed, spring pressure, friction coefficient and others.*
Key words: *mechanical seal, seal material, double cartridge, FEM analyses.*

1. INTRODUCTION

With the first mechanical seal patent, dating back to 1909, the evolution of mechanical seals has been constant, and were designed different construction types for almost every situation where needed in industry. With this increase of need for the mechanical seals, different standards made their way to regulate the construction of this equipment, but considering their complexity, the vendors will have the responsibility for their patent feasibility, as specified by the API 682 [1], the standard that is widely used when it comes to mechanical seals.

With the refinery processes having a higher demand regarding working parameters and environment than 100 years ago, the mechanical seal structure had to keep up, developing new materials for construction.

Each mechanical seal requires at least two opposing seal faces to be in contact, and they are typically categorized as either a soft against hard, or hard against hard combination, based on the type of lubrication properties [2, 3].

Soft vs. hard seal face combinations are traditionally used in boundary lubricated and mixed lubrication modes that require self-lubricating properties. The rings' face materials will be in contact with each other and good tribological pairings prevent the seal faces from causing significant damage. Hard against hard faces are typically applied in full fluid film applications, that do not necessarily require good tribological properties, since the face materials should not come into contact [2].

The lubricating properties are typically given by different factors, such as the fluid type being sealed (gas or liquid), fluid viscosity at the working temperature. The fluids that have a low viscosity tend to have a lower lubrication factor and the fluids with higher viscosity are better for lubrication. The high viscosity factor is typically reserved for the hard against hard faces [2]. Other factors that will influence the mechanical seal faces material will be temperature, rotational velocity, pressure limits etc. [2].

The scope of this paper is to analyze the changes in behavior of the contact faces pressure, based of different material couplings, considering two softs against hard cases, paired with two hard against hard pairings, all of them in dry conditions.

2. CALCULATION

As stated before, mechanical seals can be found in different structural form, a typical one being presented in Figure 1.

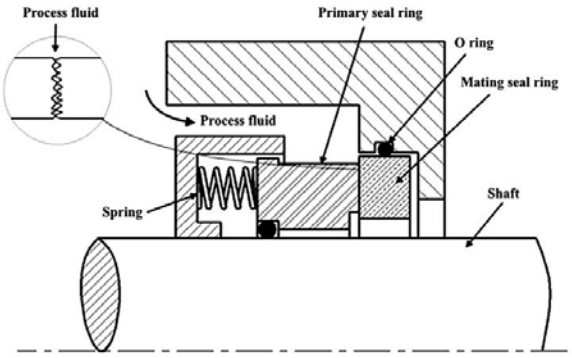

Fig 1. Mechanical seal construction, [4]

It's working procedure is straight forward, the dynamic ring, being connected to the pump shaft via sleeve, and is receiving a rotational movement, that creates a sliding effect on the static ring. For those two faces to not be opened up by the opening forces, additional springs are used to keep the equipment closed. Those three pieces are additional supported by two O-rings placed on each mating ring to make sure no leaking will take place at the joints with the shaft or at the pump housing level. Additionally, to the above-mentioned components, one or two working fluids are acting on the seal, creating both opening and closing force in addition to heat transfer.

The main request for a mechanical seal to stay close, is the opening force to be lower than the closing force [5]. Even if this request is being met, the seal will still have a low leakage rate, based on the maximum roughness of the mechanical seal material pair. There is no mechanical seal with zero leakage [1].

The opening force formula can be taken from API 682 [1], and can be seen in equation 1.

$$F_{\text{op}} = A \cdot \Delta p \cdot K, \text{[N]}. \quad (1)$$

where,

A, it is the contact face area, [mm^2]:

$$A = \frac{\pi(D_o^2 - D_i^2)}{4}. \quad (2)$$

D_o - outside diameter, [mm];

D_i - inside diameter, [mm];

Δp - pressure across the seal face, [MPa];

K - pressure drop coefficient. K, it is a number between 0 and 1 which represents the pressure drop as the sealed fluid migrates across the seal faces. For flat seal faces (parallel fluid film) and a non-flashing fluid, K it is approximately equal to 0.5, [1]. For convex seal faces (converging fluid film) or flashing fluids, K it is greater than 0.5, [1]. For concave seal faces (diverging fluid film), K it is less than 0.5, [1].

The closing force, or the contact force, can be determined from the API 682 [1], and it will consist in the equation 3:

$$p_{\text{c}} = \Delta p\ (B - K) + p_{\text{sp}}, \text{[MPa]}. \quad (3)$$

where,

B - seal balance ratio. The balance ratio value representation it is showed in the Figure 2, and the values could be calculated with relations (4.a) and (4.b);

p_{sp} - spring pressure, [MPa].

For external pressured seals (where the external pressure is higher than the barrier fluid), B it is:

$$B = \frac{D_{\text{o}}^2 - D_{\text{b}}^2}{D_{\text{o}}^2 - D_{\text{i}}^2}. \quad (4a)$$

For internal pressured seals (where the barrier fluid pressure is higher than the pump fluid pressure), B it is:

$$B = \frac{D_{\text{b}}^2 - D_{\text{i}}^2}{D_{\text{o}}^2 - D_{\text{i}}^2}. \quad (4b)$$

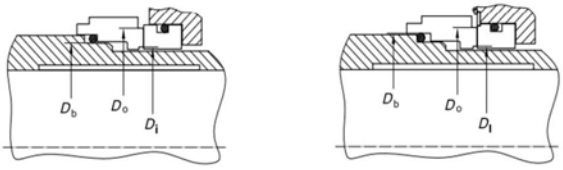

Fig. 2. Balance ratio measurement points, [1]

For obtaining the minimum contact pressure required for the seal to not leak, we will need to equalize the opening force, and contact pressure, but first, we must transform equation 1 into pressure, resulting equation 5:

$$p_{\text{op}} = \Delta p \cdot K, \text{[MPa]}. \quad (5)$$

$$p_{\text{op}} = \Delta p \cdot (B - K) + p_{\text{sp,}} \text{[MPa]}. \quad (6)$$

$$p_{\text{sp}} = p_{\text{op}} - \Delta p \cdot (B - K), \text{[MPa]}. \quad (7)$$

Considering that all of the parameters from equation 7 are based on the seal design and working parameters, except the spring pressure, we can calculate the minimum spring pressure required to achieve the smalles contact pressure possible without opening the mechanical seal.

The correct calculation of those parameter is important, as by having a high level of contact pressure, it will generate a high temperature value, that can be calculated with equation 8:

$$H = \frac{T_r \cdot N}{9550}, [\text{kW}]. \quad (8)$$

where,

T_r - running torque;

N - rotation per minute.

$$T_r = p_c \cdot A \cdot f \cdot \frac{D_m}{2000}, [N \cdot m]. \quad (9)$$

where,

D_m - mean face diameter, [mm];

f - friction coefficient.

In conformity with equations 8 and 9, the heat generated by the seal, it is directly proportional with the contact pressure, but also with the friction coefficient of the mating materials.

For the calculation in FEA, three types of materials will be paired together. The properties of the coupling materials can be found in figures 3, 4 and 5.

1. Impregnated graphite with resins→ Schunk data base [6].

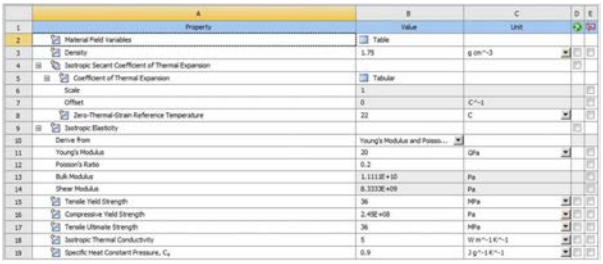

	A	B	C	D	E
1	Property	Value	Unit		
2	Material Field Variables	Table			
3	Density	1.75	g cm^-3		
4	Isotropic Secant Coefficient of Thermal Expansion				
5	Coefficient of Thermal Expansion	Tabular			
6	Scale	1			
7	Offset	0	C^-1		
8	Zero-Thermal-Strain Reference Temperature	22	C		
9	Isotropic Elasticity				
10	Derive from	Young's Modulus and Poisso...			
11	Young's Modulus	20	GPa		
12	Poisson's Ratio	0.2			
13	Bulk Modulus	1.1111E+10	Pa		
14	Shear Modulus	8.3333E+09	Pa		
15	Tensile Yield Strength	36	MPa		
16	Compressive Yield Strength	2.49E+08	Pa		
17	Tensile Ultimate Strength	36	MPa		
18	Isotropic Thermal Conductivity	5	W m^-1 K^-1		
19	Specific Heat Constant Pressure, C_p	0.9	J g^-1 K^-1		

Fig. 3. Impregnated graphite parameters

2. Silicon Carbide → Ansys Discovery data base [7].

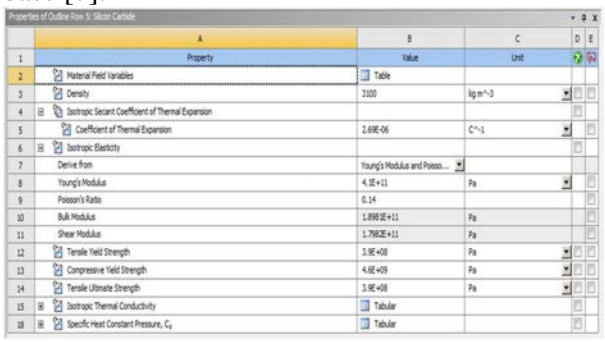

	A	B	C	D	E
1	Property	Value	Unit		
2	Material Field Variables	Table			
3	Density	3100	kg m^-3		
4	Isotropic Secant Coefficient of Thermal Expansion				
5	Coefficient of Thermal Expansion	2.69E-06	C^-1		
6	Isotropic Elasticity				
7	Derive from	Young's Modulus and Poisso...			
8	Young's Modulus	4.1E+11	Pa		
9	Poisson's Ratio	0.14			
10	Bulk Modulus	1.8981E+11	Pa		
11	Shear Modulus	1.7982E+11	Pa		
12	Tensile Yield Strength	3.9E+08	Pa		
13	Compressive Yield Strength	4.6E+09	Pa		
14	Tensile Ultimate Strength	3.9E+08	Pa		
15	Isotropic Thermal Conductivity	Tabular			
16	Specific Heat Constant Pressure, C_p	Tabular			

Fig. 4. Silicon Carbide properties

3.Tungsten Carbide → Ansys Discovery data base [7].

As stated on chapter 1 of the paper, the sealed fluid parameters, but also the mechanical pump working conditions are very important for the scope. In table 1 are presented the mechanical seal working parameters and fluid characteristics.

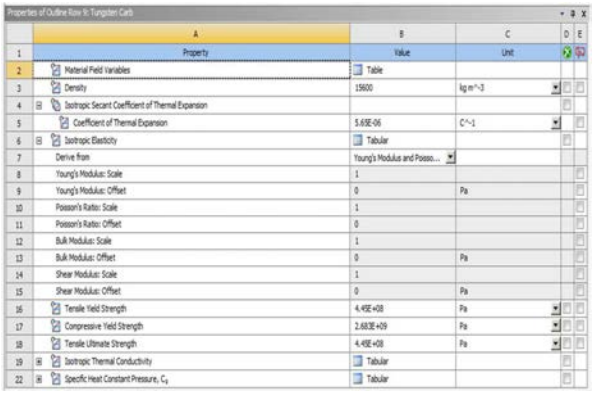

	A	B	C	D	E
1	Property	Value	Unit		
2	Material Field Variables	Table			
3	Density	15600	kg m^-3		
4	Isotropic Secant Coefficient of Thermal Expansion				
5	Coefficient of Thermal Expansion	5.65E-06	C^-1		
6	Isotropic Elasticity	Tabular			
7	Derive from	Young's Modulus and Poisso...			
8	Young's Modulus: Scale	1			
9	Young's Modulus: Offset	0	Pa		
10	Poisson's Ratio: Scale	1			
11	Poisson's Ratio: Offset	0			
12	Bulk Modulus: Scale	1			
13	Bulk Modulus: Offset	0	Pa		
14	Shear Modulus: Scale	1			
15	Shear Modulus: Offset	0	Pa		
16	Tensile Yield Strength	4.49E+08	Pa		
17	Compressive Yield Strength	2.683E+09	Pa		
18	Tensile Ultimate Strength	4.49E+08	Pa		
19	Isotropic Thermal Conductivity	Tabular			
22	Specific Heat Constant Pressure, C_p	Tabular			

Fig. 5. Tungsten Carbide properties

The dimensions of the inboard and outboard seal pairs can be found in the figure 6 and 7.

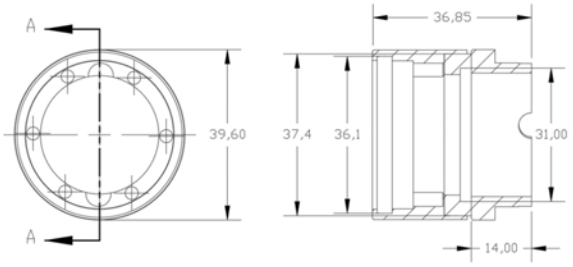

Fig. 6. Inboard seal parameters

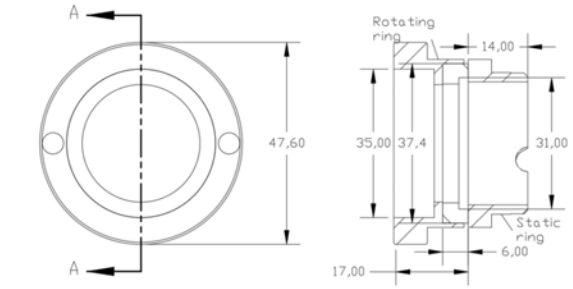

Fig. 7. Outboard seal parameters

Table 1.

Mechanical seal working parameters and characteristics.

Description	Inboard	Outboard
Working fluid pressure	0.3 MPa	-
Barrier fluid pressure on entry	0.44 MPa	0.44 MPa
Barrier fluid pressure on exit	0.40 MPa	0.40 MPa
Pump shaft speed	3000 RPM	3000 RPM
Outside diameter of the seal, D_o	37.4 mm	37.4 mm
Inside diameter of the seal, D_i	31 mm	31 mm
Balance diameter of the seal, D_b	36.1 mm	35
Pressure drop coefficient, K	0.5	0.5
Number of springs, n	6	8

All of the above information are considered from a working pump system in one of Ploiesti refineries.

Table 2.
Calculation results.

Description	Inboard	Outboard
Opening Force	24.05 N	75.60 N
Opening Pressure	0.07 MPa	0.22 MPa
Area	343.64 mm^2	343.64 mm^2
Balancing ratio	0.78	0.60
Spring Pressure	0.03056	0.1746
Spring Force	10.50	60.02
Spring force per unit	1.75	7.50

The spring calculation has been explained in the paper [8].

The values from table 2 will be used in the finite element analysis as input information. More than that, we will also require the friction coefficient between the material pairs, that will be determined in the following chapter.

3. EXPERIMENTAL DETAILS AND RESULTS

As stated before, we are dealing with a frictional contact between the rotating ring face and the static ring face, a contact that needs to be understood. For this case, we used the CMS tribometer, model TRB, presented in figure 8.

For the experiments, two rings were considered, one of tungsten carbide (figure 8), and one of silicon carbide (figure 9) as rotational sample, that got in contact with a cube type probe (3.96 x 3.96 x 4 mm) of graphite impregnated material as fixed sample.

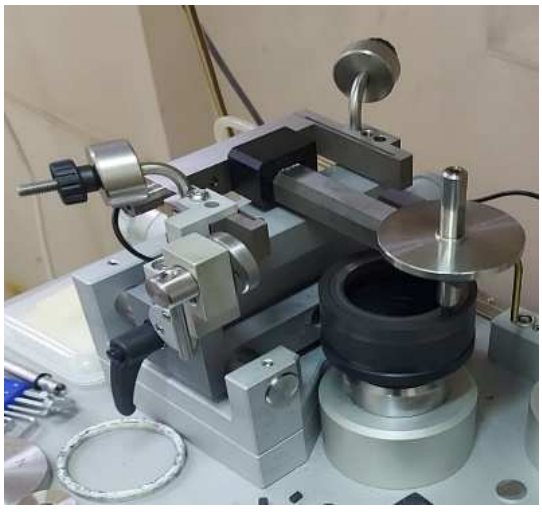

Fig. 8. CSM tribometer, model TRB

Those two rings, how can be better seen in figure 9, were in contact with a graphite impregnated with resins material, that was having a flat face in shape of a square, with the side of 3.96 mm long resulting a surface contact similar with seal rings surface contact.

The last parameter we need is the force that needs to be applied for our scope. By using the results from table 2, we can calculate the force that we need to apply for the scope to simulate the working process.

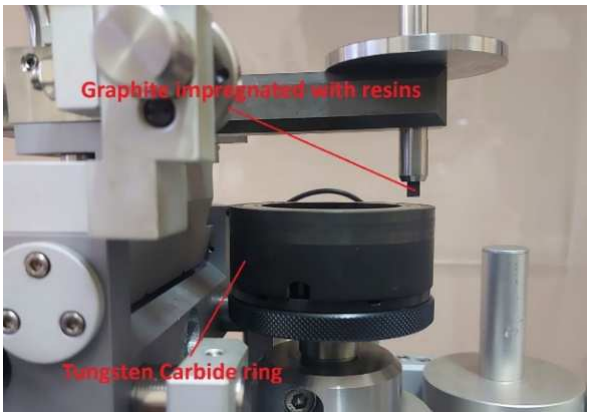

Fig. 9. WC ring mounted on CSM tribometer, model TRB

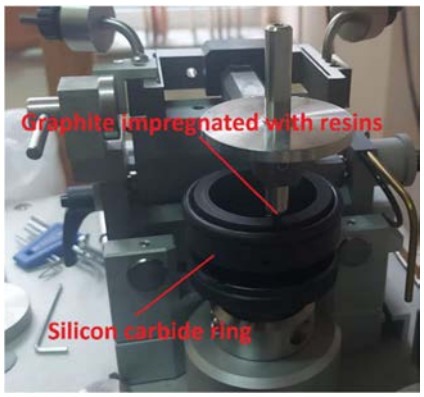

Fig. 10. SiC ring mounted on CSM tribometer, model TRB

$$p_{op} = \frac{F}{A} => F = p_{op} \cdot A, [\text{N}] \qquad (10)$$

where,

F - minimum force that needs to be applied;

A - graphite impregnated with resins contact area.

By using equation 10, it results the following:

For the inboard seal:

$$F = 0.07 \cdot 15.68 = 1.097 \text{ N}$$

For the outboard seal:

$$F = 0.22 \cdot 15.68 = 3.45 \text{ N}$$

The test was conducted by applying a normal load of 1, respectively 3.5 N, as presented in table 3. For the combination of seals SiC + WC under dry conditions, the friction coefficient was considered from S. K. Sharma, et al. study [9], but also W. Zhang, et al [10], that showed that at this materials couple, friction coefficient is situated between 0.33 and 0.66. For our case, we will consider 0.33.

Table 3. Input for CSM tribometer.

Parameter	Value
Radius	29 mm
Speed	0.5 m/s
Frictional displacement	400 m
Acquisition rate	2.7 Hz
Material 1	Graphite impregnated with resins
Material 2	Tungsten Carbide
Material 3	Silicon Carbide
Force for the inboard seal	1 N
Force applied for the outboard seal	3.5 N
Lubrication	Dry

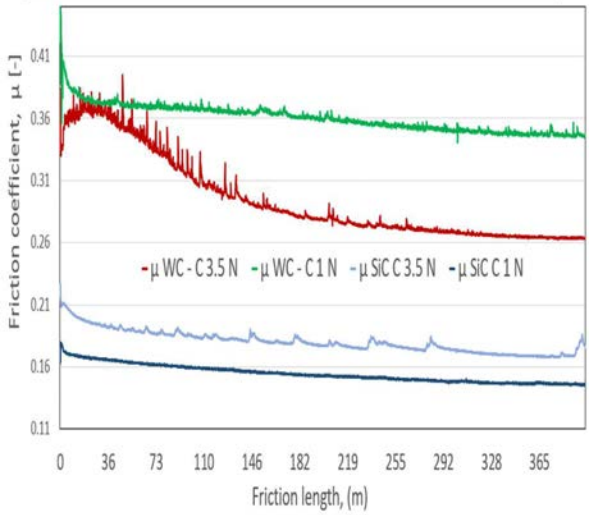

Fig. 11. Evolution of COF with friction length

Table 4.

Friction coefficient results.

Pair of materials	Normal load, *F* [N]	μ, [-]
WC + C	3.5	0.2636
	1	0.3460
SiC + C	3.5	0.1689
	1	0.1459

The values of friction coefficients were considered based on the stabilized portion of the graphic from figure 11. In figure 12 are shown the aspect of rings after tests.

Fig. 12. Faces of the two rings after testing

4. FINITE ELEMENT ANALYSIS

With the all the above information, the next step has been to create the model, based on the mechanical seal type CDSA (Cartridge Double Seal Arrangement) from Aesseal [11], that were purchased with the characteristics from figure 14.

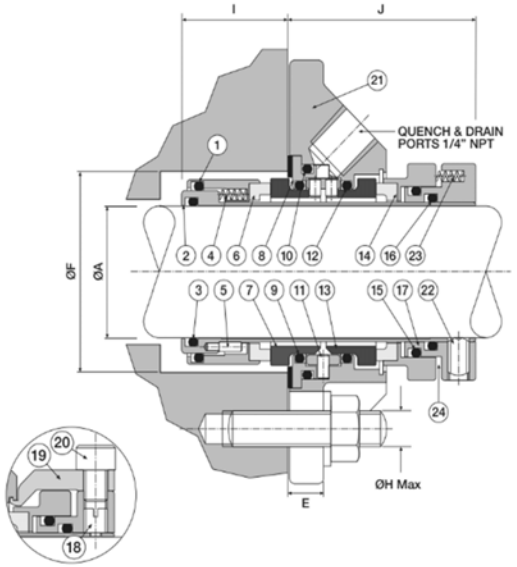

Fig. 13. Aesseal CDSA mechanical seal, [11]

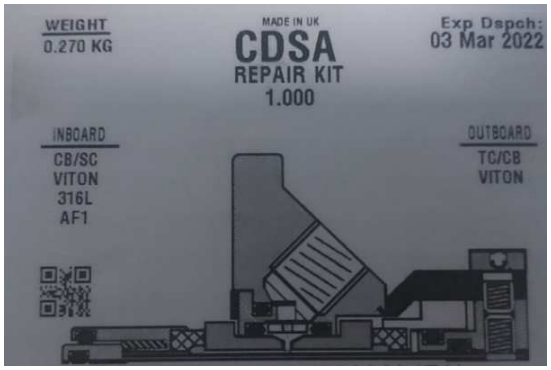

Fig. 14. Aesseal CDSA material characteristics, [11]

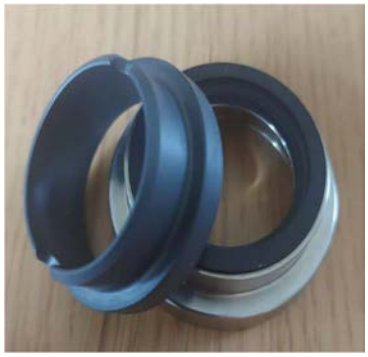

Fig. 15. Aesseal CDSA pair of rings seal

The dimensions of the two seals can be found in figure 6 and 7, with the material parameters being found on figures 3, 4 and 5, resulting in the models shown in figure 16.

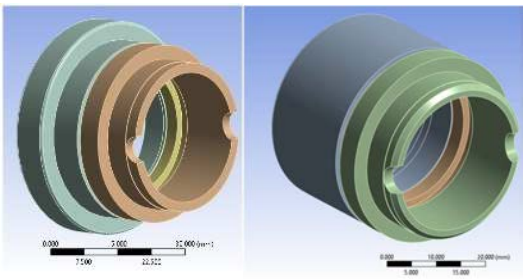

Fig. 16. FEA components

Worth mentioning, is the fact that the two components that are in contact, are also supported by another body, constructed from 316L SS.

The two pieces that are forming the rotating ring, are considered in Ansys as having a bonded contact, with the contact surfaces presented in figure 17.

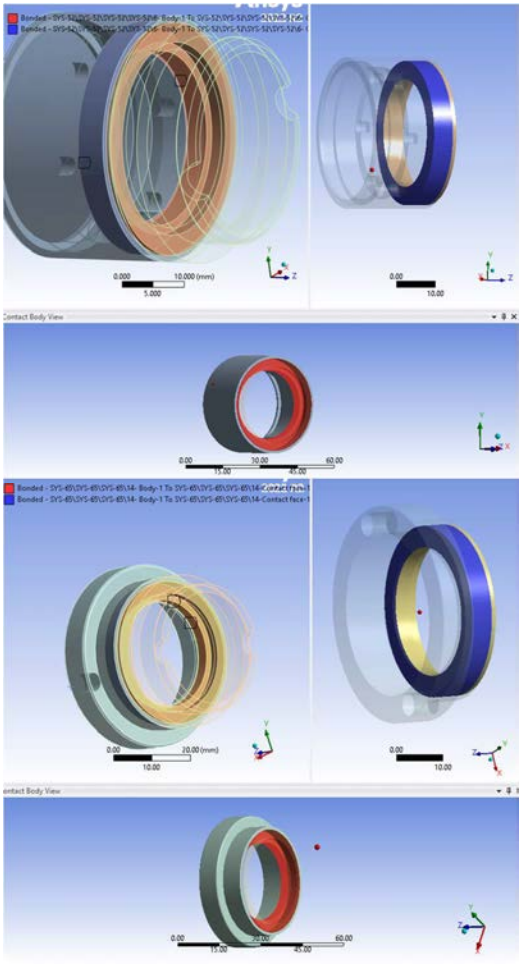

Fig. 17. Bonded contact inside the rotating ring

On the other side, for the contact between the static and rotating ring, a frictional contact will be considered, with the coefficient of friction obtained from figure 11 / table 4.

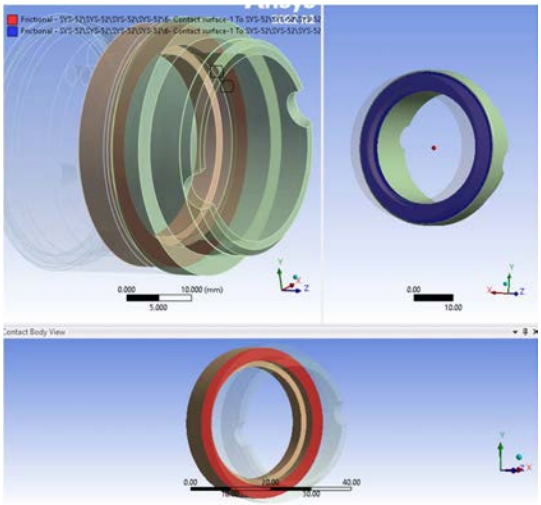

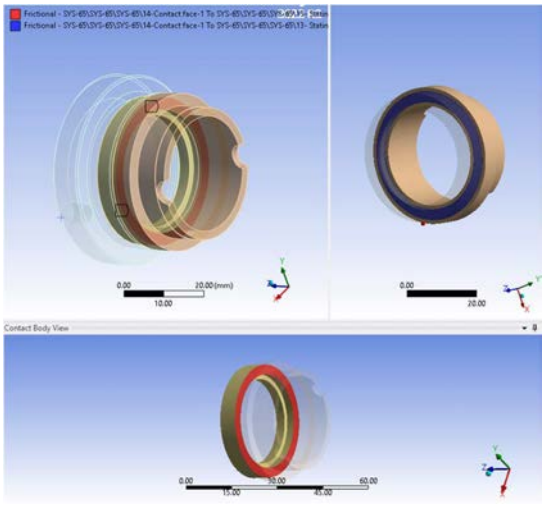

Fig. 18. Frictional contact between the two rings

Table 5. Discretization values.

Parameter	Inboard	Outboard
Dynamic ring body mesh	0.8 mm	0.8 mm
Dynamic ring contact body mesh	0.5 mm	0.5 mm
Static ring mesh	0.8 mm	0.8 mm
Refinement on both contact face	Level 2	Level 2
Refinement on spring acting surface	Level 1	N/A
Mesh Type	Hex Dominant Method All Quad	
Elements	1088044	703125
Nodes	1448475	1088044

The mesh structure was considered by taking values step by step, analyzing the habits of the seal, but also the running time. In the end, the following values presented in table 5 were considered:

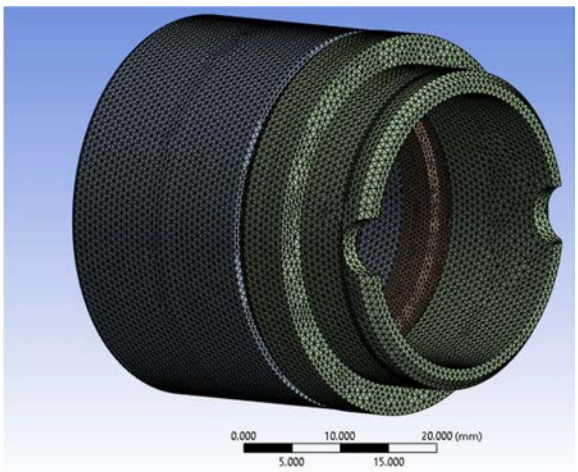

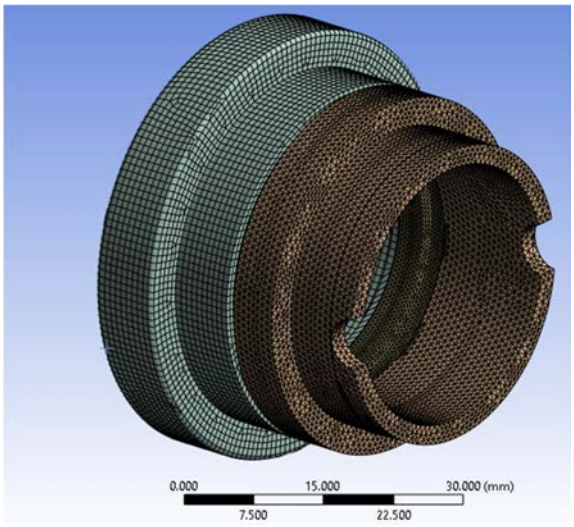

Fig. 19. Mesh distribution on the seals

The difference between the two seals on nodes and elements is mainly due to structural reasons, the inboard seal being more complex, and with a higher volume.

All the data required for the input information has been previously discussed, except the pressure that is acting on the seal pair. The areas that are subject to pressure is in figure 21.

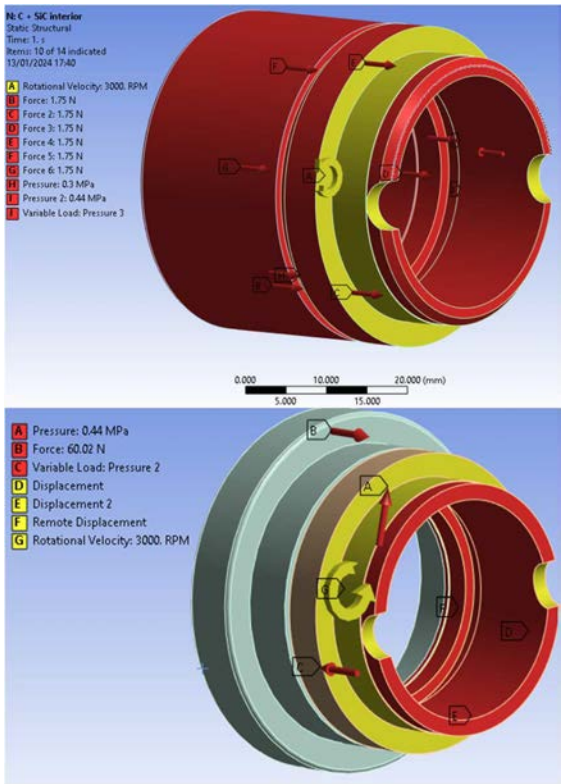

Fig. 20. Seal inputs

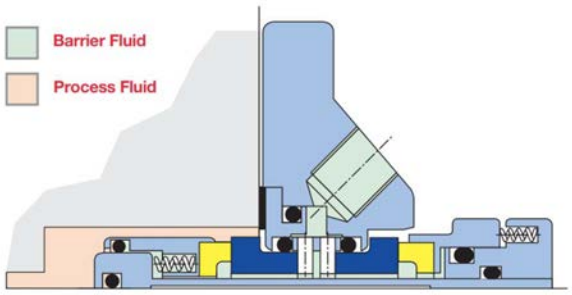

Fig. 21. Faces subject to pressure on the CDSA mechanical seal

Both internal and external pressures are given in table 1, but for the barrier fluid pressure, the pressure flow was checked using the Ansys Fluent, and the results can be found in figure 22.

As observed on the mentioned figure, the pressure inside the seal varies between 0.4 MPa to 0.44 MPa, but for keeping a more conservative approach, the inside pressure was considered 0.44 MPa.

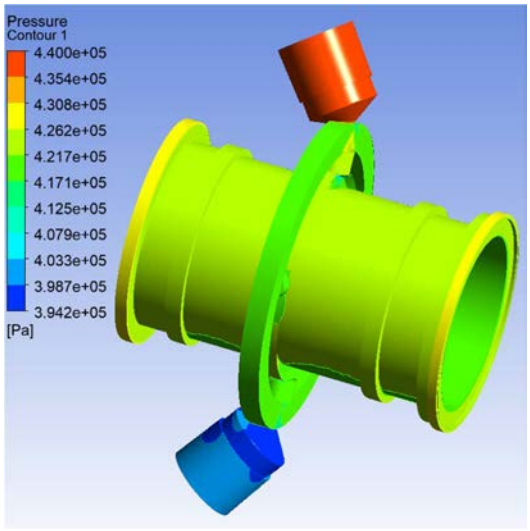

Fig. 22. The pressure of barrier fluid

The pressure that has the biggest role in opening the seal face is represented by the interstitial pressure. This pressure represents the pressure between the two faces and has a linear distribution, from the inside pressure value to the external pressure, as presented in figure 23.

5. RESULTS

With the support of Ansys structural, the following contact pressure distribution were obtained:

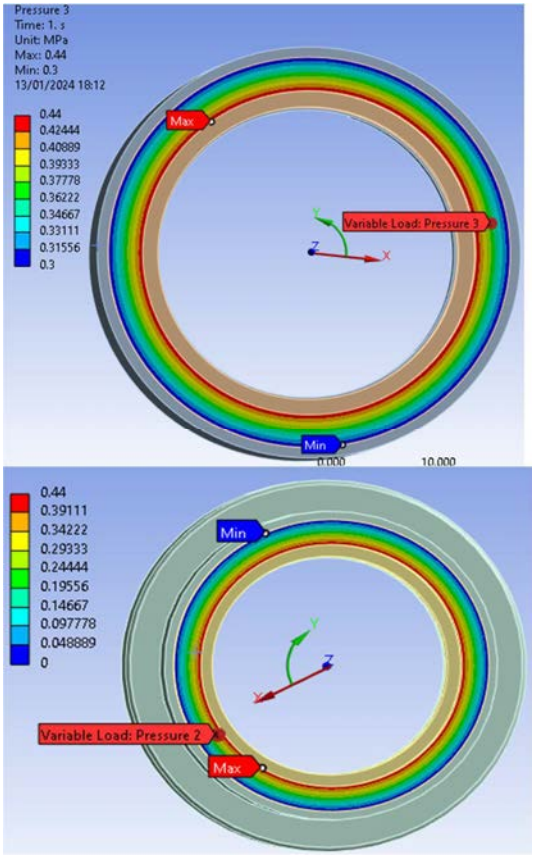

Fig. 23. Interstitial pressure

The first contact discussed will be the one between silicon carbide and the graphite impregnated with resins, a contact between a soft face and a hard face, under dry lubrification. On this case, we can see the pressure distribution of both rings, in figure 24 and 25.

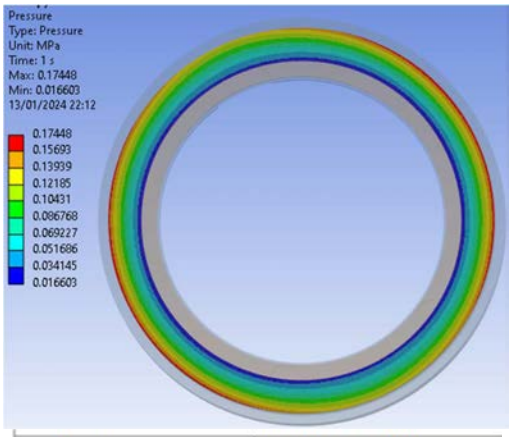

Fig. 24. Inboard C + SiC contact pressure

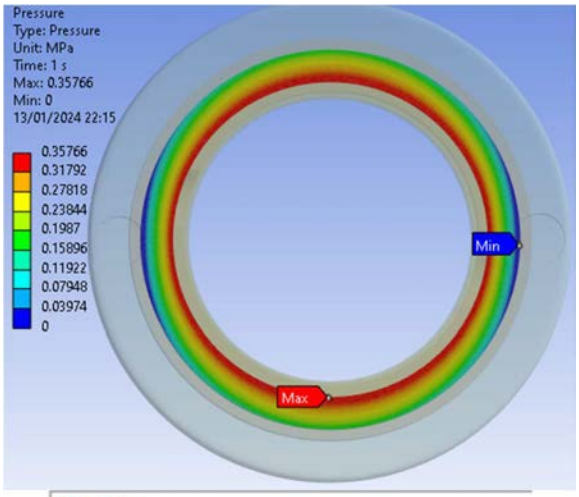

Results	
Minimum	0. MPa
Maximum	0.35766 MPa
Average	0.23306 MPa

Fig. 25. Outboard C + SiC contact pressure

As a result of materials characteristics, the contact is close to linear, with permanent contact between the seals. For the inboard combination, as presented in figure 14, this was the go-by-choose by the vendor for this application, even if it is having a higher contact pressure than is required, but it makes sure that the leakage level is on a lower value.

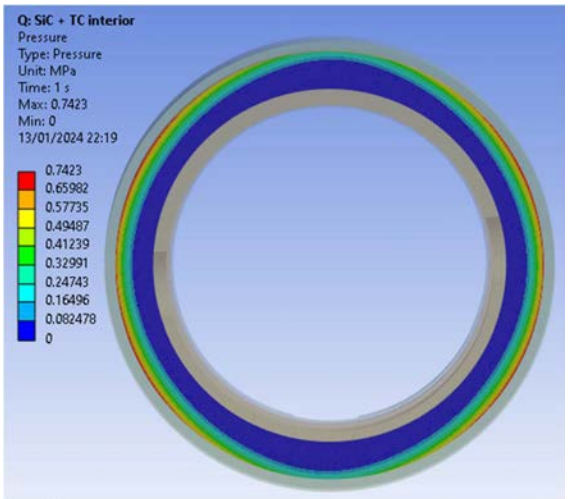

Minimum	0. MPa
Maximum	0.7423 MPa
Average	0.1552 MPa

Fig. 26. Inboard SiC + WC contact pressure

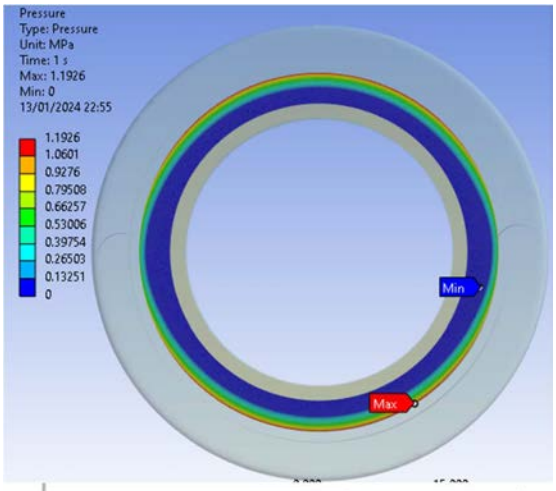

Minimum	0. MPa
Maximum	1.1926 MPa
Average	0.24126 MPa

Fig. 27. Outboard SiC + WC contact pressure

It can be seen from the start, in this, due to material combination, the seal is having a low contact point, this being due to deformation. As the seal is pushed by the spring and additional pressure, the material will have to absorb the force, but due to the hard structure of both materials, this type of absorption is not possible. In figure 28, we can see the deformation that the rotating ring is having, while getting into contact with the static tungsten carbide ring.

This configuration will generate extensive wear on the exterior side of the seal, creating an uneven contact surface in the end.

One way to resolve this situation is to have a good lubrification film, between the two seals, high enough to absorb the impact, as additionally confirmed by W. Dietzel et al. [2].

In the following step, we will present the opposite of the above, with Tungsten carbide as contact face for the rotating ring, and Silicon carbide as static ring. With this change being done, we can see that the contact pressure is a bit more robust, having the maximum value lower than on previous case, with Silicon carbide being a bit softer than Tungsten carbide, and being able to deform, helping the contact, as presented in the figure 29 and 30.

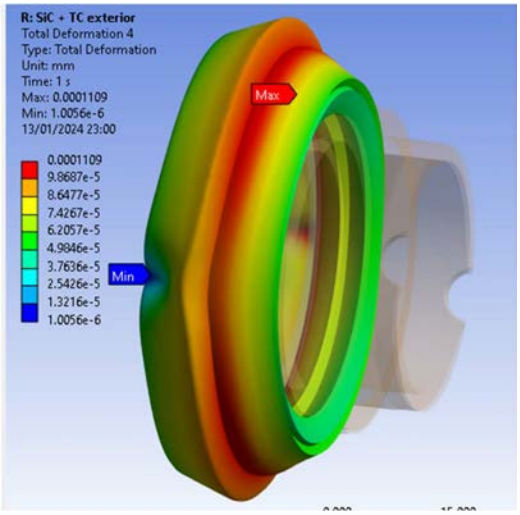

Fig. 28. Outboard rotating ring from SiC deformation under scale

The final topic that is going to be discussed is the contact between the graphite impregnated with resins as rotating ring and tungsten carbide as static ring. This is the most benefic between the four cases presented, as this is the one having the softest face in contact with the hardest one.

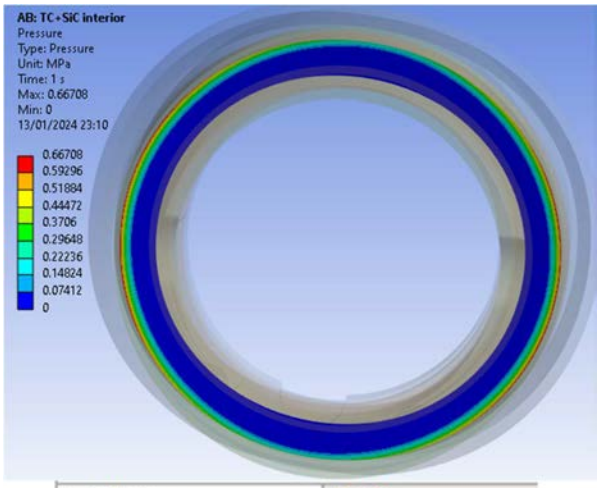

Fig. 29. Inboard WC + SiC contact pressure

As can be seen from figure 31, the minimum and maximum range are lower, and the average pressure is very close to what the minimum required value from the standard is, 0.07 MPa.

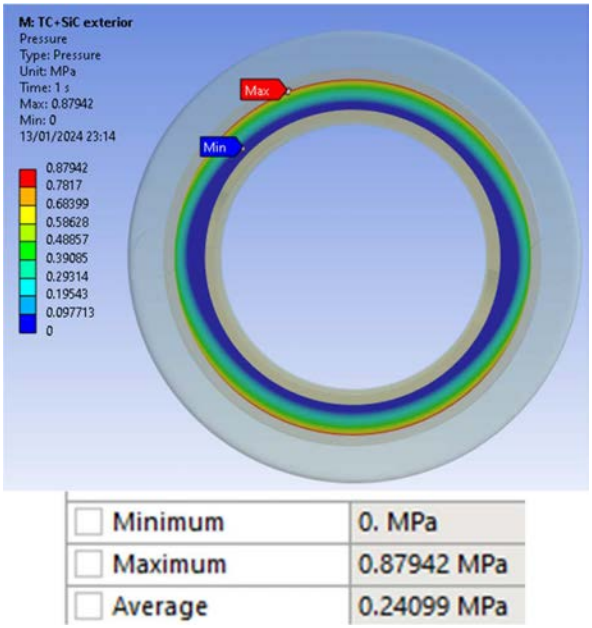

Fig. 30. Outboard SiC + WC contact pressure

On the other hand, the outboard seal is as close as possible to the minimum value given by the standard, and once more with a more constant distribution of pressure on the seal faced, than on the first case. This option, for the outboard seal, was considered by the vendor for this type of seal.

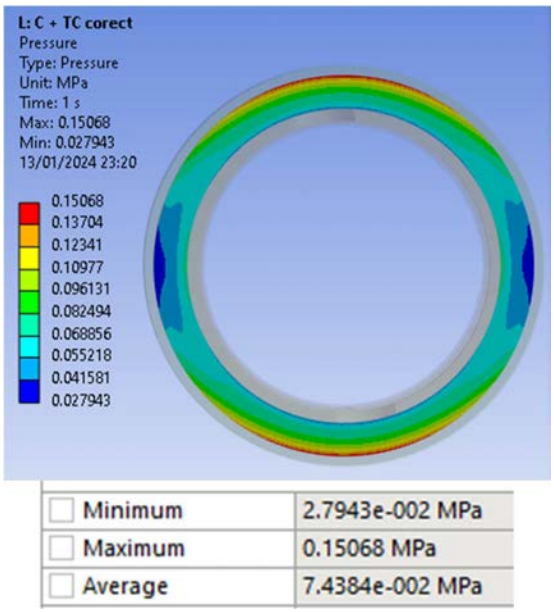

Fig. 31. Inboard C + WC contact pressure

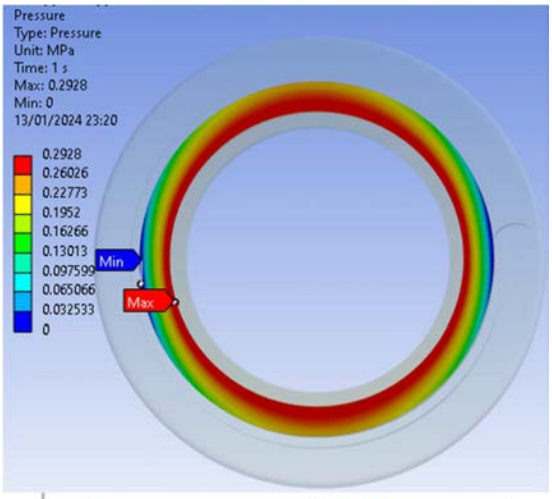

Fig. 32. Outboard C + WC contact pressure

6. CONCLUSIONS

Mechanical seals are critical equipment for the durability of the dynamic equipment in refinery, with them becoming more complex every day.

The paper presents the importance of choosing the correct material based on the working parameters of the pump, and the fluid film that is being generated by the seal.

As can be seen in table 6, when we are talking about a the hard against hard faces (SiC + WC and WC +SiC), we can see an increased value in pressure (fig. 26, 27, 29 and 30), due to mechanical characteristics. This increase in contact pressure is generating additional heat, almost double in some cases that the soft against hard surface, a heat that in time is going to generate wear, that is going to reduce the lifespan of the mechanical seal.

Table 6. Results values.

Material pair	Inboard pressure [MPa]	Outboard pressure [MPa]
C + SiC	0.08531	0.2336
SiC + WC	0.1552	0.2416
WC + SiC	0.09381	0.24099
C + WC	0.07438	0.22145

As mentioned in the paper, the calculations consider dry running, for which, the heat and wear will increase. In the second phase we are moving to the wet running, the friction coefficient will go down, and also there will be a small dampener into the frictional contact, resulting in a better absorption of force, than the one considered in figure 28.

For the outboard seal, the contact pressure is not having so great difference, due to the missing component of the working fluid, as it is only acted by the barrier fluid. This is creating a more controlled environment, but the contact pressure is still with ~10% higher for the hard vs hard seal surface then soft against hard faces.

We need to keep in mind, that the maximum pressure value is going to influence the behavior of the seal as well, in some areas, due to increase contact pressure, the seal will suffer a temperature increase, causing uneven wear to the faces.

7. BIBLIOGRAPHY

[1] API Standard 682, 2014, *Pumps—Shaft Sealing Systems for Centrifugal and Rotary Pumps.*

[2] Dietzel W., Vasko J., *The evolution and application of mechanical seal face materials*, https://hdl.handle.net/1969.1/162203.

[3] Kavinprasad S., Shankar S. and Karthic M., 2015, Industrial Lubrication and Tribology, *Experimental and CFD investigations of carbon/SS316 mechanical face seals under different lubricating conditions*, 67(2), 124-132 https://doi.org/10.1108/ILT-03-2013-0037.

[4] https://www.researchgate.net/figure/Fig-1-Mechanical-seal-major-components_fig1_261596351, accessed at 28.12.2023.

[5] Pana I., Preda I., 2002 **Mechanical seals** (in Romanian), Ed. University of Petroleum and Gas, Ploiesti, pp. 20-25.

[6] https://www.schunk-group.com/en, accessed at 28.12.2023

[7] https://www.ansys.com/products/3d-design/ansys-discovery accessed at 28.12.2023

[8] Stanciu A., Ilinca C., Ripeanu R.G., 2023, Tribology in Industry, *Design of the springs tightening for a double cartridge mechanical seal*, 45(4), 718-728.

[9] Sharma, S.K., Manoj Kumar, B.V. & Kim, *YW*, 2019, Friction, *Tribology of WC reinforced SiC ceramics: Influence of counterbody,* 7(2), 129–142. https://doi.org/10.1007/s40544-017-0194-2

[10] Zhang W, Yamashita S., Kita H., 2020, Materials & Design, *Progress in tribological research of SiC ceramics in unlubricated sliding-A review*,190, 108528. https://doi.org/10.1016/j.matdes.2020.108528.

[11] https://www.aesseal.com/, accessed at 28.12.2023.

Analiza influenței materialelor inelelor de contact și a condițiilor de lucru asupra presiunii de contact într-o etanșare mecanică dublă tip cartuș

Abstract: Articolul prezintă cum presiunea de contact la suprafața celor două inele ale etansarii variază în funcție de diferite materiale, cum ar fi grafitul impregnat cu rășini, carbura de siliciu sau carbura de wolfram, pentru o etanșare dublă tip cartuș, utilizând calculul cu element finit. În funcție de perechea materialelor ce intră în contact, comportamentul presiunii de contact dintre fețe se schimbă, datorită capacității materialelor de a se deforma, a absorbi tensiunea, dar și din cauza forțelor de frecare. Parametrii considerați în etanșare, pe lângă presiunea interioară și exterioară au fost, turațiile arborelui pompei, presiunea arcurilor, coeficientul de frecare etc.

Andrei STANCIU, Ph.D. Student Eng, Petroleum-Gas University of Ploiesti, Romania, andrei.stanciu@upg-ploiesti.ro

Razvan George RIPEANU, Prof. Univ. Dr. Eng. Habil., Petroleum-Gas University of Ploiesti, Romania, rrapeanu@upg-ploiesti.ro